Original Research Article

ENERGETICS OF THE BASIC ALLOTROPES OF CARBON

ABSTRACT

An effort was made in this work to calculate the total ground state energy and electronic band structure of Fullerenes (C_{60}), Graphite and Diamond using FHI-aims Density Functional Theory (DFT) code. The density functionals used are the local-density approximation (LDA) in the parameterization by Perdew and Wang 1992, Perdew and Zunger 1981, the generalized gradient functional PBE, and PBE+vdW approach as defined by Tkatchenko and Scheffler. The results obtained from the computations of the ground state energies of diamond, fullerenes and graphite were -2072.569 eV, -1027.178 eV and -2070.938 eV respectively. These results agrees well when compared to the various exchange and correlation functionals used in this study. Similarly, the results obtained from the computations of the Kohn Sham electronic band gaps of graphite and diamond were 0.00072eV and 5.57611eV, respectively. These are also in agreement when compared to the experimental values of 0eV and 5.45eV. These band gaps are within reasonable overestimation errors of 0.0% and 1.43% respectively. However, fullerenes band gap of 8.21131eV is not in agreement with theoretical and experimental values of 1.83eV and 2.3eV, respectively. This is probably due to the Bucky-ball nature of Fullerenes as well as the lattice constants and physical settings used.

Keywords: DFT, LDA, GGA, Band Gap, HOMO, LUMO and Total Ground state Energy.

1. INTRODUCTION

Carbon is found naturally in the earth crust and in the atmosphere. It is abundant and forms a major part of our life. Carbon is a unique and versatile element. It exists in many forms with different structures and properties. It can also be synthesized to form new forms of materials [1]. Carbon is the basic building block of the following Carbon materials: graphite, diamond, fullerene, graphene, Carbon-fiber, Carbon nanotube, lonsdaleite, carbyne and buckydiamonds. Recently, new Carbon form called penta-graphene was discovered using Vienna Ab initio Simulation Package (VASP) [2]. Similarly, novamene [3] was also discovered and the stable equilibrium structure was computed using

Quantum Espresso code. The ability of Carbon to exist in many forms with different structures and properties led researchers into a rigorous research on Carbon nanomaterial.

The principal allotropes of Carbon are graphite, diamond and Fullerenes. Diamond is associated with the sp^3 hybrid orbital, all four electrons are used to form a tetravalent sigma σ bond in a 3D structure. In each unit cell, diamond has eight Carbon atoms. The bond length is equidistant between the four Carbon atoms, thereby forming a strong covalent bond with bond angle of 109.5^0. Diamond is the hardest known material, it is used in cutting, drilling and grinding. It is transparent in the visible range of the electromagnetic spectrum, making it a good candidate for jewelry. It has a high thermal conductivity (more than copper) and low thermal expansion [1 and 4]

Graphite has a flat layered (planar) structure. Each Carbon atom forms trivalent (sigma σ) bond with three (sp^2 hybrid orbital) other Carbon atoms in a hexagonal shape. The layers are bonded to one another by weak Van-der-Waal forces. This allows the layers to slip over each other. The p_z – orbitals electrons, do also interact: they form a π-mobile electron. Graphite is the most stable and most strongly covalently bonded Carbon allotrope (within the layer). It is soft, opaque, black, used in pencil, lubrication and in nuclear reactor moderator [1 and 4].

In recent time, a new Carbon allotrope was discovered by Curl, Kroto and Smalley at Rice University. It is spherical (soccer ball) in shape. It resembles a geodesic dome constructed by an architect in person of Richard Buckminster Fuller. Hence, it was named in his honour as buckminsterfullerene, shortened as fullerenes (also called buckyballs). It has sixty (60) Carbon atoms arranged in both pentagonal and hexagonal shape. For it to have a spherical shape, it must satisfy the pentagon rule i.e. it must have 12 pentagons and 20 hexagons. Basic Fullerene molecular formula is C_{60} [1 and 4]. Unlike graphite and diamond, fullerene molecule has both sp^3 and sp^2 hybrid orbitals, i.e., It has both sigma and pi bond. Fullerene is used as a high temperature superconductor when doped with K or Rb, it is a possible lubricating aid and is also used in medicine [1 and 5].

Nowadays, Density Functional Theory (DFT) is one of the leading tools used in studying the electronic structure, stability, synthesis, defects, semiconducting and superconducting properties of Carbon materials. DFT is a special computational quantum mechanical first principle method of describing and predicting the electronic structures and properties of atoms, molecules and solids. [19] *used DFT GAUSSIAN 3 software to* compute the ground state energies and stable structures of diamond, graphite and fullerenes. [20] calculated the stable atomic structure of fullerenes using FHI-aims code.

They reported that the most stable structure crystallizes in fcc structure. This crystal structure was used in this study for fullerenes computations.

In this work, using FHI-aims DFT package [6] structural units of Carbon basic allotropes were simulated.

2. MATERIAL AND METHODS

First principles, or *ab initio* calculations represent the pinnacle of electronic structure calculations. Starting with the fundamental constants and Schrodinger's equation as a postulate, these methods proceed to describe the nature of atomistic systems to a degree that is almost irrefutable. The methods applied in solving Schrodinger's equation break into two main types: Hartree-Fock (HF) based methods and Density Functional Theory (DFT) methods. While both make approximations to make calculations possible, they represent the best available methods for atomistic modeling. The first task is to have a Linux based operating system (0S) (Ubuntu 16.04 version installed for this research work) on a computer. FHI-aims (Fritz Haber Institute-*ab* initio molecular simulations) is not supported on windows. Since FHI-aims is distributed in source code form, the next task is to compile a powerful executable program. For this, the following mandatory prerequisites are needed [6]:

• A working FORTRAN compiler. A good example is Intel's ifort compiler.

• A compiled version of the lapack library, and a library providing optimized basic linear algebra subroutines (BLAS). Standard commercial libraries such as Intel's mkl provide both lapack and BLAS support. Having an optimized BLAS library for a specific computer system is critical for the performance of FHI-aims.

FHI-aims requires two input files — control.in and geometry.in—located in the same directory from where the FHI-aims binary is invoked. An output file contains the basic information and result of the calculation such as the total energy, atomic forces, etc. The geometry.in file contains all information concerning the atomic structure of the system. This includes the nuclear coordinates, which are specified by the keyword; atom, followed by Cartesian coordinates (in units of Å) and the descriptor of the species (chemical elements) [7].The control.in file contains all other physical and technical settings for accurate and efficient convergence of the computations.

The full algorithmic framework embodied in the FHI-aims computer program package is described in [6]. The algorithms are based on numerically tabulated atom-centered orbitals (NAOs) to capture a wide range of molecular and materials properties from quantum-mechanical first principles. FHI-aims is a very important code because, an all-electron / full-potential treatment that is both computationally efficient and accurate is achieved for periodic and cluster geometries on equal footing, including relaxation and *ab initio* molecular dynamics. The primary production method for total energies and gradients is density functional theory (LDA and GGA). Additional functionality includes quantum-chemical approaches (Hartree-Fock, hybrid functionals, MP2) and self-energy-based methods (e.g., GW) for electronic spectroscopic properties. FHI-aims allows fully quantum-mechanical simulations for systems up to thousands of atoms, and performs efficiently also on massively parallel platforms with possibly thousands of CPUs [6].

However, choosing the central computational settings consistently for series of calculations greatly enhances the accuracy of any resulting energy differences (error cancellation). In FHI-aims, the key parameters regarding computational accuracy are actually sub-keywords of the species keyword of control.in, controlling the basis set, all integration grids, and the accuracy of the Hartree potential. These settings of course were not retyped from scratch for every single calculation; on the other hand, they remained obvious, since these are the central handles to determine the accuracy and efficiency of a given calculation.

FHI-aims therefore provides preconstructed default definitions for the important sub-keywords associated with different species from *Z*=1-102 (H-Md). These can be found in the *species_defaults* subdirectory of the distribution, and are built for inclusion into a control.in file by simple copy-paste.

For all elements, FHI-aims offers three different levels of *species_defaults*, however we used only two of these levels of species_defaults in this work:

• *light* : Out-of-the-box settings for fast pre-relaxations, structure searches, etc. Actually, no obvious geometry / convergence errors resulted from these settings, and are recommended for many household tasks. For “final” results (meV-level converged energy differences between large molecular structures etc.), any results from the *light* level should be verified with more accurate post-processing calculations, e.g. *tight*.

• *tight* : Regarding the integration grids, Hartree potential, and basis cutoff potentials, the settings specified here are rather safe, intended to provide meV-level accurate energy *differences* also for

large structures. In the *tight* settings, the basis set level is set to *tier* 2 for the light elements 1-10, a modified *tier* 1 for the slightly heavier Al, Si, P, S, Cl (the first *spdfgd* radial functions are enabled by default), and *tier* 1 for all other elements. This reflects the fact that, for heavy elements, *tier* 1 is sufficient for tightly converged ground state properties in DFT-LDA/GGA, but for the light elements (H-Ne), *tier* 2 is, e.g., required for meV-level converged energy differences. For convergence purposes, the specification of the basis set itself (*tier* 1, *tier* 2, etc.) may still be decreased / increased as needed [6].

2.1 COMPUTATIONAL DETAILS

Various computations were done for the pw_lda, pz_lda and pbe_GGA XC functionals. The Gaussian occupation broadening width of 0.01eV was selected. The convergence criterion for the SCF of eigenvalues, total energy and density were set to 10^{-2}eV, 10^{-5}eV and 10^{-4}eV, respectively. The structure geometry with a convergence minimum of 10^{-2}eV was optimized, while for the unit cell geometry optimization we selected full unit cell relaxation option. The corresponding convergence criteria for the SCF of the energy derivatives was chosen to be 10^{-4}eV.

Tier 1 basis functions of FHI-aims light species_default basis set was used for the geometry optimization, however, tier 2 tight basis set was used for the post relaxation of the relaxed geometry. BFGS (Broyden, Fletcher, Goldfarb and Shanno) structure optimization algorithm was selected for the geometry relaxation. FHI-aims keyword k_grid was set to 12x12x12 k_grid data point. For the long range correlation energy interaction effect, we used VdW correction based on Tkatchenko and Scheffler long range interaction correction.

3. RESULTS AND DISCUSSION

The following tables summarize the output data obtained during FHI-aims computations, and are used in discussing the minimum and stable ground state energies for the relaxed/post relaxed computations of the various XC functionals for the three bulk structures.

Table 4.1: Diamond Ground State Energies for Relaxed/Post Relaxed Computations.

Functionals Computations	Pw_lda Ground State Energy (eV)	Pz_lda Ground State Energy (eV)	Pbe (GGA) Ground State Energy (eV)

Relaxed Geometry (Light)	-2056.94097548	-2056.90780088	-2072.47722687
Postrelaxed Geometry (Tight)	-2057.03098622	-2056.99760599	-2072.56851605

From table 4.1, it can be observe that pbe XC functional has the minimum ground state energy for diamond bulk structure. This is in agreement with theory, because pbe (GGA) is theoretically a better approximation to XC energy functional than the rest LDA and LSDA [8 and 9]. However, pw_lda is a bit better approximation when compared to pz_lda. Similarly, comparing light and tight FHI-aims species_default settings for relaxed and postrelaxed computations, tight gives an efficient and accurate converged ground state energies than the light settings. This is a good indication that diamond crystalline structure has been well optimized in the relaxed/postrelaxed FHI-aims computations. The following graphs summarize the output data obtained during FHI-aims computations, and are used in obtaining the binding curve pattern for the total energy and the number of iterations.

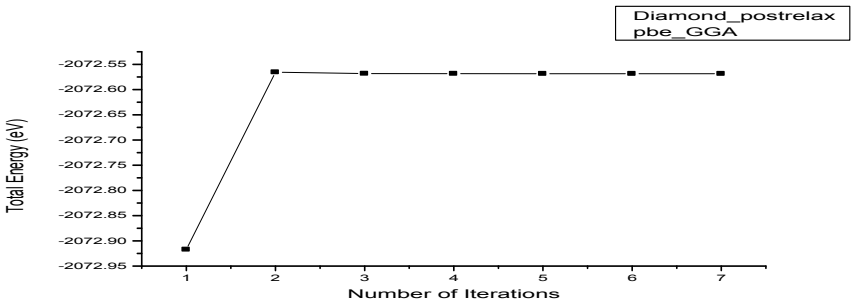

Fig. 4.1: Variations of Total Energy (eV) against Number of Iterations

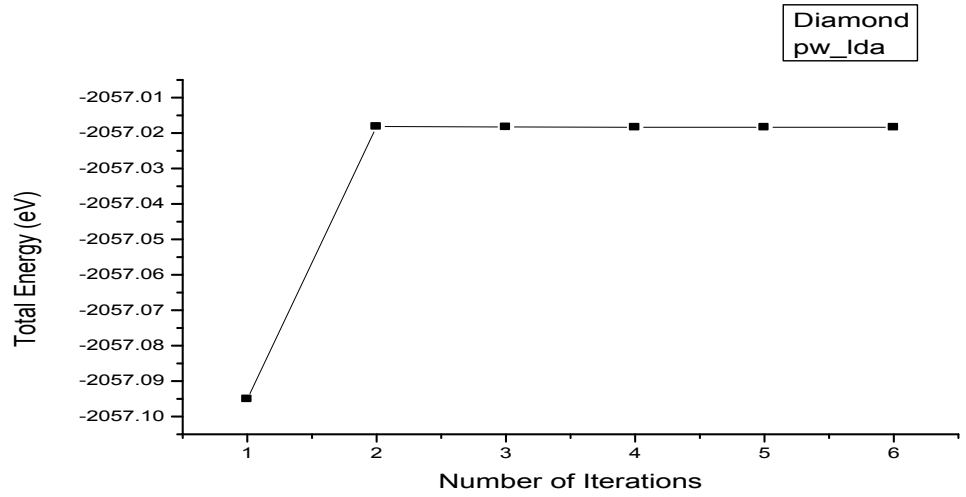

145

146 Fig. 4.2: Variations of Total Energy (eV) against Number of Iterations.

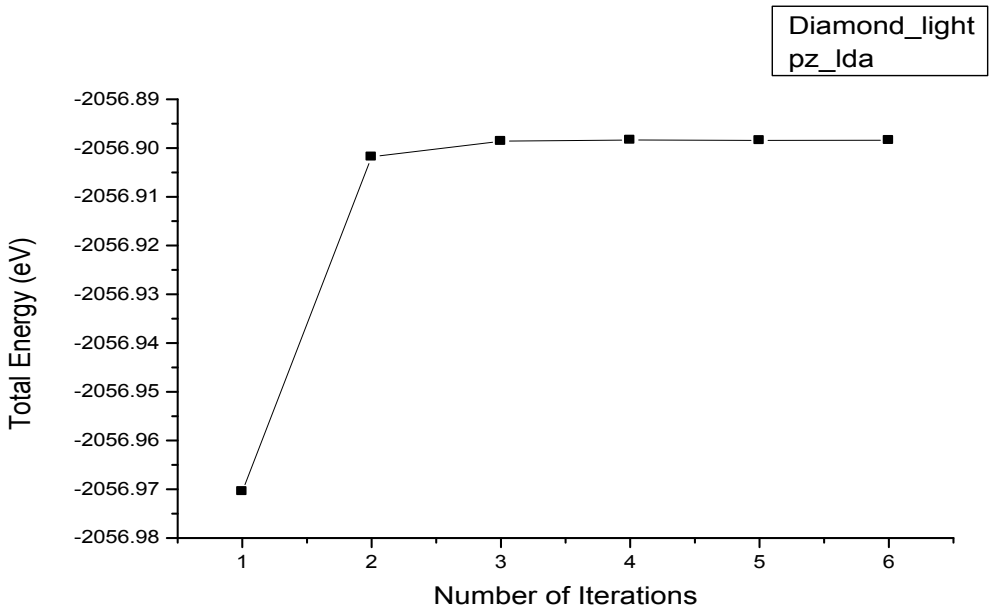

147

148 Fig. 4.3: Variations of Total Energy (eV) against Number of Iterations.

149 The binding curve in Fig. 4.1 shows that the total energy of the bulk crystal of diamond increases as
150 the number of iteration increases and converges steadily. The resulting binding curve indicates a
151 stable total energy and also the best converged energy of -2072.56851605eV for diamond. This
152 variation pattern for diamond total energy against the number of iterations was found to be the same
153 for the remaining XC functionals used in this study.

Fig. 4.2 and Fig. 4.3 also illustrate the variations of diamond's ground state energies against the number of iterations. It is clear that the graphs variations are almost the same, except that the total energies values are different. In Fig. 4.2 graph, the total energy value increases steadily from the 1st iteration to the 2nd iteration, from where this value decreases a bit and is later maintained until convergence is reached. However, fig. 4.3 shows a slight different trend. The total energy value rather increases in the third iteration, this value was maintained until convergence was obtained. The resulting binding curve in Fig. 4.3 indicates a stable total energy and also the best converged energy of -2056.89840811eV for diamond.

Table 4.2: Graphite Ground State Energies for Relaxed/Post Relaxed Computations

Functionals Computations	Pw_lda Ground State Energy (eV)	Pz_lda Ground State Energy (eV)	Pbe (GGA) Ground State Energy (eV)
Relaxed Geometry (Light)	-2044.81236553	-2044.81251118	-2061.63381564
Postrelaxed Geometry (Tight)	-2054.61937938	-2054.63065901	-2070.93836837

From table 4.2, it can be observe that pbe XC functional also has the minimum ground state energy for graphite bulk structure. This is in agreement with theory, because pbe (GGA) is theoretically a better approximation to XC energy than the rest pw_lda and pz_lda [9]. However, pw_lda is slightly a better approximation when compared to pz_lda. Similarly, comparing light and tight species_default settings for relaxed and postrelaxed computations, tight gives an efficient and accurate converged ground state energies than the light settings. This is also a good indication that graphite crystalline structure has been well optimized in the relaxed/postrelaxed FHI-aims computations.

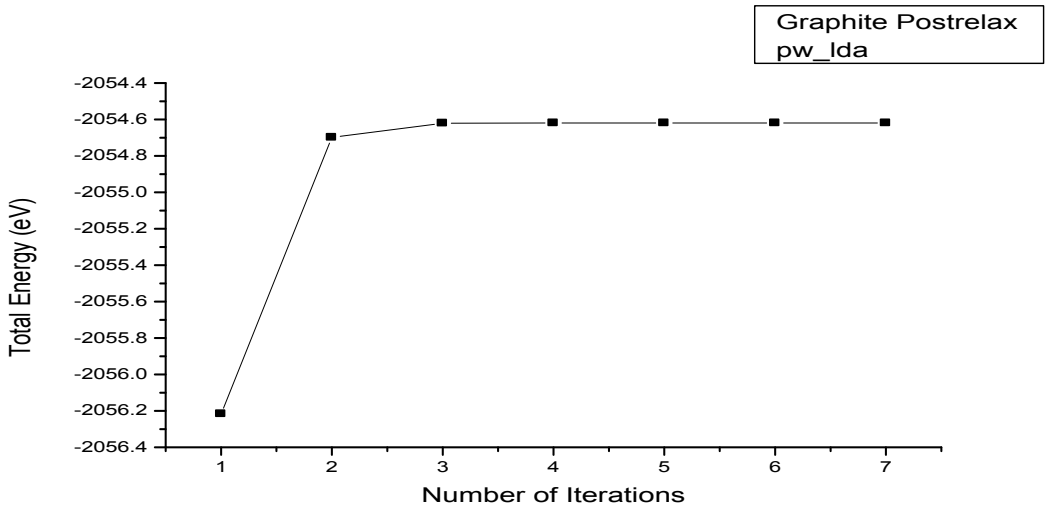

171

172 Fig. 4.4: Variations of Total Energy (eV) against Number of Iterations.

173

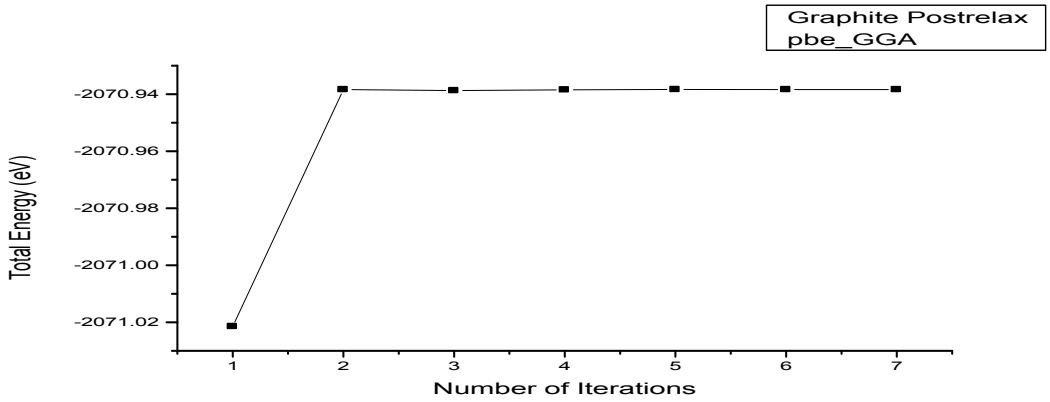

174

175 Fig. 4.5: Variations of Total Energy (eV) against Number of Iterations.

176 Fig. 4.4 and Fig. 4.5 illustrate the variations of ground state energies against number of iterations for
177 graphite bulk structure. The trend in both Figures increases upwardly to create a curve pattern until it
178 reaches stability at the 3rd, 4th, 5th, 6th and 7th iterations, this can be attributed to the covalent bonding
179 and simple planar hexagonal stacking that exist in the bulk atom of graphite [10]. The resulting
180 binding curve in Fig. 4.5 indicates a stable total energy and also the best converged energy of -
181 2070.93836837 eV for graphite.

182

183

184 Table 4.3: Fullerenes Ground State Energies for Light and Tight Settings.

Functionals Computations	Pw_lda Ground State Energy (eV)	Pz_lda Ground State Energy (eV)	Pbe (GGA) Ground State Energy (eV)
Light	-1018.35981067	-1018.35683745	-1027.17026568
Tight	-1018.36680612	-1018.36379535	-1027.17849607

For Fullerenes, ground state energies for relaxed/postrelaxed computations were not successful, because FHI-aims could not write out the geometry.in_next_step file let alone post relax processing. We suggest this could be due to the dimension of fullerenes lattice constant of 14.17A^{o}, physical settings used and/or its spherical shape However, we computed the ground state energies for light/tight settings without structure optimization. Table 4.3 shows fullerenes ground state energies for the three XC functionals using light/tight default settings. The table also shows that, tight default settings gives a more accurate converged minimum ground state energy when compared to the light default settings. This is in good agreement with the theory behind FHI-aims code [6]. Also looking at the XC functional total energy values, it is obvious that pbe gives the minimum ground state energy follow by pw_lda and then pz_lda. Hence, in accordance with theory pbe is much better in approximating the XC energy functional than pw_lda and pz_lda [8 and 9].

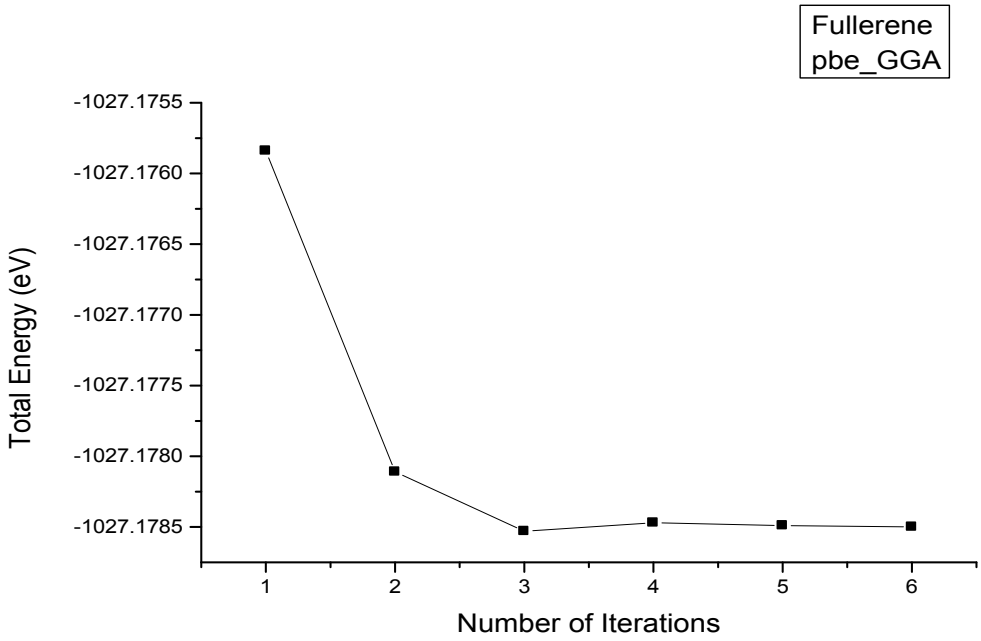

Fig. 4.6: Variations of Total Energy (eV) against Number of Iterations.

Figure 4.6 illustrates the variations of Fullerenes ground state energies for the pbe XC functionals against number of iterations. The trend in Fig. 4.6 decreases downwardly to create a curve pattern until it becomes stable at the 4^{th}, 5^{th} and 6^{th} iterations, this can be attributed to the covalent bonding and spherical shape that exist in the bulk atom of fullerenes [10 and 11].

In this paper, we find out that all the three variants of the total energy from FHI-aims output file are the same for diamond structure but are all different in the case of graphite and fullerenes. This shows that fullerenes and graphite have narrow and zero HOMO-LUMO gap respectively, while diamond has a wide HOMO-LUMO gap. These results are in good agreement with experimental and theoretical literatures [10 and 12]. Tables 4.4-4.6 show estimated values for lowest unoccupied state (CBM), highest occupied state (VBM), overall HOMO-LUMO gap and smallest direct gap for diamond, graphite and fullerenes as obtained from the three XC functionals used in this study.

Table 4.4: Diamond Electronic Band Structure for Postrelaxed Computations

Functionals Bands	Pw_lda Ground State Energy (eV)	Pz_lda Ground State Energy (eV)	Pbe (GGA) Ground State Energy (eV)
Valence Band Maxima (VBM)	-8.54310497	-8.53387243	-8.10988403
Conduction Band Minima (CBM)	-4.34300078	-4.34356041	-3.95778618
HOMO-LUMO Gap	4.20010419	4.19031201	4.15209785
Smallest Direct Gap	5.61457427	5.60711319	5.57611325

From table 4.4, using the estimated overall HOMO-LUMO gap, FHI-aims code predicted that diamond appears to be an indirect band gap. This agrees well with the report of Pierson, 1993. The smallest direct gap of 5.57611325eV for pbe_GGA is in good agreement with theoretical and experimental values [10 and 21] with an overestimation percentage error of 1.43%. According to FHI-aims output file, since the gap value is above 0.2eV, the system is most likely an insulator or a semiconductor. This FHI-aims output file comment agrees exactly with theoretical and experimental data. Diamond was characterized in many literatures to be an insulator [4], however, it was also considered as an

indirect wide band gab semiconductor [1] that is suitable for high temperature electronic applications. The rest XC functionals pw_lda and pz_lda Smallest Direct Gap are also in good agreement with experimental values of 5.5eV [10] with an overestimation error of 1.96%.

Table 4.5: Graphite Electronic Band Structure for Postrelaxed Computations

Functionals Bands	Pw_lda Ground State Energy (eV)	Pz_lda Ground State Energy (eV)	Pbe (GGA) Ground State Energy (eV)
Valence Band Maxima (VBM)	-7.07415413	-7.33934792	-6.81313445
Conduction Band Minima (CBM)	-7.06569011	-7.33861834	-6.80852692
HOMO-LUMO Gap	0.00846402	0.00072958	0.00460753
Smallest Direct Gap	0.21308645	0.41541884	0.30724683

From table 4.5, using the estimated overall HOMO-LUMO gap, FHI-aims predicted that graphite also appears to be an indirect band gap. The smallest direct gap of 0.21308645eV for pw_lda is in good agreement with theoretical [13] and experimental values [10]. According to FHI-aims output file, since the HOMP-LUMO gap value (0.00072958eV) is rather small (approximately zero gap) and we use a finite k-point grid, the material is most likely metallic in the sense that there are states at or near the Fermi level. This FHI-aims output comment shows that graphite is a conductor, and it agrees exactly with theoretical [13] and experimental data . Also, the approximately zero gap value of FHI-aims output file is in agreement with the literature [10]. The rest XC functionals pz_lda and pbe_GGA Smallest Direct Gap are also in good agreement with experimental values within small overestimation percentage errors.

Table 4.6: Fullerenes Electronic Band Structure for Tight Settings Computations

Functionals Bands	Pw_lda Ground State Energy (eV)	Pz_lda Ground State Energy (eV)	Pbe (GGA) Ground State Energy (eV)
Valence Band Maxima (VBM)	-13.60248641	-13.60706560	-13.71228408
Conduction Band	-5.39117210	-5.39539613	-5.25904269

Minima (CBM)			
HOMO-LUMO Gap	8.21131431	8.21166947	8.45324138
Smallest Direct Gap	8.21131432	8.21166948	8.45324139

From table 4.6, using the estimated overall HOMO-LUMO gap, FHI-aims predicted that fullerenes also appears to be an indirect band gap. The smallest direct gap of 8.21131432eV for pw_lda and the remaining XC functionals values do not agree with theoretical value of 1.83eV [12] and experimental value of 2.3eV [Byun 2012, PhD Dissertation, Pennsylvania State University]. According to FHI-aims output file, since the gap value is above 0.2 eV. The system is most likely an insulator or a semiconductor. This FHI-aims output prediction agrees exactly with theoretical and experimental data, fullerenes was reported to be a band insulator, direct band-gap semiconductor [1]. In addition, fullerenes can be converted from a semiconductor into a conductor or even superconductor when doped with alkali metals [14]. The rest XC functionals pz_lda and pbe_GGA Smallest Direct Gap are also not in good agreement with theoretical [12] and experimental values.

It can be easily observed that all the electronic band gaps above are overestimated by certain percentage errors. This is because generally, DFT overestimates the band gap energy of solids [8].

5. CONCLUSION

The total ground state energy and electronic band structure of Fullerenes (C_{60}) for University]. According to FHI-aims output file, since the gap value is 2 eV. The system is most likely an insulator or a semiconductor. This FHI-aims output prediction agrees exactly with theoretical and experimental data, Fullerenes was reported to be a band insulator, direct band-gap semiconductor above 0. [1]. In addition, fullerenes can be converted from a semiconductor into a conductor or even superconductor when doped with alkali metals [14]. FCC, Graphite for hcp and Diamond crystal were calculated using the local-density approximation (LDA) in the parameterization by [15-17], and PBE+vdW approach as defined by [18]. The results of the total energy required for binding/stability of the ground state during the optimized process were found to converge faster with the 12x12x12 k-grid points in the Brillouin zone of the FHI-aims code. Similarly, FHI-aims tight/postrelaxed settings were found to give more accurate converged results. In terms of the XC functionals, pbe_GGA was better in approximating the XC energy functional than LDA. The result presented above have confirmed a faster and more accurate prediction of the electronic band structure and total energies of solids considered when compared to literature report of other studies reporting similar band gaps and/or total energies. Major

findings of this research are; Graphite is a zero gap conductor (0.00072958eV), diamond is a wide band gap semiconductor (5.57611325eV). These are in good agreement with experimental values of 0eV and 5.45eV, respectively. However, fullerenes is also a wide band gap semiconductor (8.21131431eV). This band gap does not agree with what was obtainable in the literature (1.83eV and 2.3eV). This discrepancy might probably be due to the present DFT calculations of the solid fullerene's lattice constant, spherical shape and the optimized parameters used in the study.

Conversely, Graphite is a suitable candidate for optoelectronic and other electronic devices. Diamond is suitable for high temperature thermal electronic devices, while fullerenes is a good material for conversion into conductors and superconductors.

REFERENCES

1. Pierson H. O.. *Handbook of Carbon, Graphite, Diamond and Fullerenes.* Noyes Publications, New Mexico; 1993.

2. Shunhong Z., Jian Z., Qian W., Xiaoshuang C., Yoshiyuki K., and Puru J., Penta- graphene: A new carbon allotrope . *PNAS,* 2014; 112(8): 2372–2377.

3. Larry A., Al Fasim M., Richard S.W., Francesco D., and Nicola M. Novamene: A new Class of Carbon Allotropes. Materials Science, Chemistry, *Heliyon 3*. 2017; 3(2): DOI: 10.1016/j.heliyon.2017.e00242.

4. Adams W. and Williams L. *Nanotechnology Dymistyfied.* United States of America:Mcgraw Hill; 2007.

5. Patrizia C., Gerald G and A. M. Koster. First-Principle Calculations of Large Fullerenes. *Journal of Chemical Theory and Compution.* 2009; *5:* 29-32.

6. Blum V., Gehrke R., Hanke F., Havu P., Havu V., Ren X., Reuter K., and Matthias S. *Ab Initio* Molecular Simulations with Numeric Atom-Centered Orbitals. Comp. Phys. Commun. 2009; 180 (11): 2175–2196.

7. Viktor A., Oliver H., and Sergey L. *Hands-On Tutorial on Ab Initio Molecular Simulations,Tutorial I: Basics of Electronic-Structure Theory.* Berlin, Fritz-Haber-Institut der Max-Planck-Gesellschaft. 2011.

290 **8.** Parr, R. G. and Yang, W. Density-Functional Theory of Atoms and Molecules. Oxford
291 University Press: New York. 1989.

292 **9.** Fiolhais C., F. Nogueira, and M. Marques (Eds.) A Primer in Density Functional Theory. Vol.
293 620, Springer-Verlag, Berlin. 2003.

294 **10.** *Krueger A.* Carbon Materials and Nanotechnology. WILEY-VCH Verlag GmbH & Co. KGaA,
295 Weinheim. 2010.

296 **11.** Fleming R. M., B. Hessen, T. Siegrist, A. R. Kortan, P. Marsh, R. Tycko, G. Dabbagh, and R.
297 C. Haddon, Fullerenes: Synthesis, Properties, and Chemistry, Chapter 2: Crystalline
298 Fullerenes. AT&T Bell Laboratories, Murray Hill, NJ 07974. 1992.

299 **12.** Heggie M. I., M. Terrones, B. R. Eggen, G. Jungnickel, R. Jones, C. D. Latham, P. R. Briddon
300 and H. Terrones. Quantitative Density Functional Study of Nested Fullerenes. *Physical*
301 *Review B, Condensed Matter and Materials Physics*. 1998; 57(21): 13339-13342.

302 **13.** Charlier J.-C. X. Gonze and J.-P. Michenaud. First-Principles Study of the Stacking
303 Effect on the Electronic Properties of Graphite(S) . *Carbon.* 1994; *Vol. 32, No. 2*:
304 289-299.

305 **14.** *Katz, E. A. Fullerene Thin Films as Photovoltaic Material. In Sōga, Tetsuo.* Nanostructured
306 materials for solar energy conversion. *Elsevier. 2006;361–443. ISBN 978-0-444-52844-5.*
307 **15.** Perdew, J.P. and Wang, Y. Accurate and Simple Analytic Representation of the Electron-Gas
308 Correlation Energy. *Physical Review B*, 1992; 45(23): 13244-13249.
309 http://dx.doi.org/10.1103/PhysRevB.45.13244.
310 **16.** Perdew, J.P. and Zunger, A. Self-Interaction Correction to Density-Functional Approximations
311 for Many-Electron Systems. *Physical Review B*. 1981; **23**, 5048-5079.
312 http://dx.doi.org/10.1103/PhysRevB.23.5048.
313 **17.** Perdew J. P., K. Burke, and M. Ernzerhof. Generalized gradient approximation made simple.
314 Phys. Rev. Letter. 1997; 77 (18): 3865–3868.
315 **18.** Tkatchenko A. and M. Scheffler. Accurate molecular van der Waals interactions from ground
316 state electron density and free-atom reference data. Physical review letters. 2009; 102(7),
317 073005. DOI: 10.1103/PhysRevLett.102.073005.

19. J. M. González, A. Ruden, C. Barbosa, C. Ortega and F. Sequeda. Computational Study of Allotropic Structures of Carbon by Density Functional Theory (DTF). Ingeniería y Ciencia . 2014; 10(19):145–162. http://www.eafit.edu.co/ingciencia.

20. Abdu S.G., Adamu M.A, and Onimisi M.Y., DFT COMPUTATIONS OF THE LATTICE CONSTANT, STABLE ATOMIC STRUCTURE AND THE GROUND STATE ENERGY PER ATOM OF FULLERENES (C60). Science World Journal. 2018; 13(1): www.scienceworldjournal.org.

21. Belenkov E. A, Brzhezinskaya M.M, and Greshnyakov VA. Crystalline structure and properties of diamond-like materials. Nanosystems: Physics, Chemistry, Mathematics. 2017;8(1):127-136. DOI: 10.17586/2220805420178112713 6.